of histamine by heparin derivatives and other glycosaminoglycans to determine the minimum requirements of the imidazolium binding site.

Acknowledgment. This research was supported in part by National Institutes of Health Grant AI 24216 and by the University of California, Riverside, Committee on Research. The NMR instrumentation was supported in part by BRSG 2 S07 RR07010-20 awarded by Biomedical Research Resources, National Institutes of Health. D.L.R. thanks Professor David Lagunoff for stimulating his interest in the heparin-histamine system.

Registry No. EDA, 107-15-3; PDA, 109-76-2; BDA, 110-60-1; (IdoA-2S)-(1→4)-(GlcNSO$_3$-6S), 76149-63-8; heparin, 9005-49-6; histamine, 51-45-6; imidazole, 288-32-4; methylamine, 74-89-5; *N*-acetylhistamine, 673-49-4.

Spin and Reaction Dynamics in Flexible Polymethylene Biradicals As Studied by EPR, NMR, and Optical Spectroscopy and Magnetic Field Effects. Measurements and Mechanisms of Scalar Electron Spin-Spin Coupling

Gerhard L. Closs,*,†,‡ Malcolm D. E. Forbes,†,§ and Piotr Piotrowiak†,‡,⊥

Contribution from the Department of Chemistry, The University of Chicago, Chicago, Illinois 60637, and Chemistry Division, Argonne National Laboratory, Argonne, Illinois 60439.
Received October 1, 1991

Abstract: A series of spectroscopic measurements on flexible polymethylene biradicals in liquid solution is reported. Time resolved electron paramagnetic resonance, chemically induced nuclear spin polarization, transient optical absorption, and external magnetic field effects on lifetimes are used to unravel the kinetics of two types of biradical, acyl-alkyl and bisalkyl, obtained from the photoinduced Norrish type I α-cleavage reaction of permethylated cycloalkanones. A kinetic picture for the biradical exit channels is presented which includes rate constants for spin-orbit coupling, decarbonylation, spin relaxation, and end-to-end contact of the chains. The relative merit of each of the various experimental techniques is discussed, and the close relationship between spin and chain dynamics in the biradical kinetics is clearly illustrated. Direct and indirect measurements of the singlet-triplet splitting (electronic spin-spin coupling) are made and compared for different chain lengths. The mechanism of the coupling as well as its temperature dependence is discussed in terms of through-bond and through-space models. The acyl-alkyl biradicals are shown to have kinetics dominated by spin-orbit coupling, whereas the bisalkyl biradical spectra decay on a slower time scale via spin relaxation. Optical measurement of the decarbonylation rate of the pivaloyl monoradical is also reported.

Introduction

There has been a long standing interest in the chemistry of polymethylene biradicals in these laboratories ever since the first observation of CIDNP upon α-cleavage of cyclic ketones.[1] The recent development of time-resolved electron paramagnetic resonance (EPR) spectroscopy allowing the observation of such biradicals directly at room temperature in liquid solution, under conditions of maximum reactivity, has made it possible to gain new insight on how the reaction dynamics are governed by magnetic parameters.[2] In this paper we wish to present the results of studies on two series of biradicals obtained by EPR, NMR, transient optical absorption, and magnetic field effects on reaction rates. From these studies has emerged a unified picture of the kinetics, plus a better understanding of the relationship between spin and chain dynamics in flexible biradicals.

Before presenting the details of the present study, it will be useful to summarize a few of the previous investigations of biradical kinetics from this and other laboratories. The earliest reported experiments on spectroscopic properties of polymethylene type biradical reactions are the CIDNP investigations of Closs and Doubleday.[1] By using Norrish type I photochemical cleavage of cyclic ketones, they generated acyl-alkyl biradicals and observed the CIDNP spectra of their reaction products. Magnetic field dependence of those signals gave information on the exchange interaction in the biradicals when interpreted with theoretical models. The most complete model used to interpret these data was developed by de Kanter et al.,[3] yielding the parameters for the exponential distance dependence of the exchange coupling constant with which much subsequent work has been explained. Doubleday and Turro with their collaborators[4] used α- and α'-phenylated cyclic ketones for the purpose of providing an optical chromophore, thus making it possible to study the biradicals directly using transient absorption to obtain kinetic data. Development of submicrosecond time resolved CIDNP experiments by Closs, Miller, and Redwine[5] yielded additional kinetic information, particularly on nuclear spin dependent chemical reaction rates. Johnston and Scaiano have recently published a comprehensive review of optical studies on short biradicals (1,6 and shorter), many of them performed in their own laboratories, showing the broad spectrum of lifetimes these intermediates can cover.[6]

All these experiments have in common that the biradicals are generated from a triplet excited ketone and therefore are born with triplet spin functions. The final products of the reactions

† The University of Chicago.
‡ Argonne National Laboratory.
§ Present address: Department of Chemistry, University of North Carolina, Chapel Hill, NC 27599-3290.
⊥ Present address: Department of Chemistry, University of New Orleans, New Orleans, LA 70148.

(1) Closs, G. L.; Doubleday, C. E., Jr. *J. Am. Chem. Soc.* **1972**, *94*, 9248.
(2) Closs, G. L.; Forbes, M. D. E. *J. Am. Chem. Soc.* **1987**, *109*, 6185.
(3) de Kanter, F. J. J.; den Hollander, J. A.; Huizer, A. H.; Kaptein, R. *Mol. Phys.* **1977**, *34*, 857.
(4) Doubleday, C., Jr.; Turro, N. J.; Wang, J. F. *Acc. Chem. Res.* **1989**, *22*, 199.
(5) Closs, G. L.; Miller, R. J.; Redwine, O. D. *Acc. Chem. Res.* **1985**, *18*, 196.
(6) Johnston, L. J.; Scaiano, J. C. *Chem. Rev.* **1989**, *89*, 521.

0002-7863/92/1514-3285$03.00/0

Scheme I

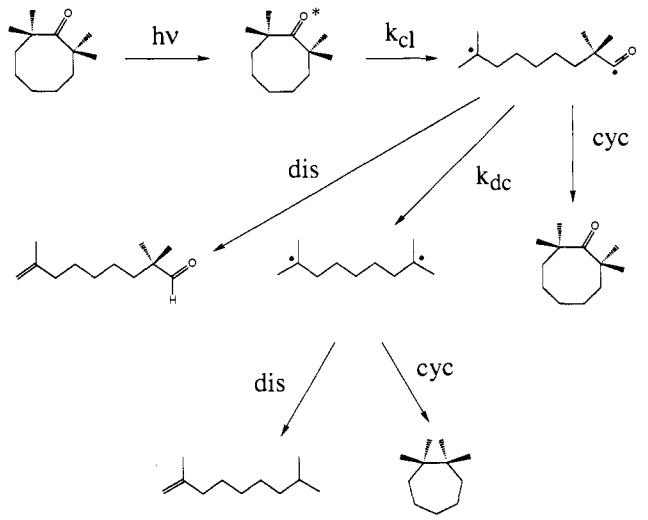

are molecules in their ground singlet states resulting from reactive encounters of the two radical sites in the biradicals. The mechanistic problem can therefore be broken down into two components, one dealing with spin dynamics leading from triplet to singlet wave functions and the other addressing the chain dynamics of the polymethylene chains. A successful model must incorporate both factors in a quantitative way. As usual, more than one experimental technique is necessary to obtain a satisfactory amount of information.

The Chemical Reaction Scheme

The generation of the biradicals was accomplished in all experiments by laser flash photolysis induced Norrish type I cleavage of cyclic ketones, presented for a representative example in Scheme I. It is well known that the cleavage reaction proceeds predominantly from the triplet excited state of the ketone and that it is thermally activated.[7] A consequence of the slow cleavage is the undesirable side reaction of transannular hydrogen abstraction which becomes predominant in medium sized and larger rings.[8] Alkylation at the α-position of the carbonyl compound lowers the activation energy for the cleavage and can eliminate the hydrogen abstraction altogether. The resulting acyl–alkyl biradical will react by either disproportionation (dis) or cyclization (cyc) to give diamagnetic products, or it can decarbonylate to yield a bisalkyl biradical which once again can yield diamagnetic products by disproportionation or cyclization. The decarbonylation, a spin independent step, is thermally activated and facilitated by alkyl substituents located at the α-carbon next to the carbonyl group. If one wants to study the dynamics of the bisalkyl biradicals, it is advantageous to peralkylate the α-positions of the cyclic ketones, thus facilitating both ring cleavage and decarbonylation. Most of the experiments reported in this paper were therefore performed on tetramethylated cyclic ketones.

It is useful to outline the kinetics to be expected for the reaction sequence shown in Scheme I. Among the reactions shown, the kinetics of the cleavage and decarbonylation steps can be expected to follow straightforward unimolecular rates with rate constants k_{cl} and k_{dc}, respectively. No determination of k_{cl} has been attempted in this work except to ensure that in our systems the reaction is fast compared to the other steps. Estimates of k_{dc} have been made and are presented below. Even without distinguishing between disproportionation and cyclization, the rate processes of product formation from either the acyl–alkyl or the bisalkyl biradicals are complicated and cannot be expressed by a single unimolecular rate constant. For each nondegenerate electronic (w) and nuclear (i) sublevel, the rate constant for product formation can in principle be different. The spin dependent rate constant for the formation of product from biradical x will be designated as ${}^{x}k^{w}_{i}$. This is the sum of a nuclear spin independent component which is assumed to be identical for all electron spin states, k_{so} (for spin–orbit coupling), and the rate processes which depend on spin wave function properties such as the degree of singlet character ${}^{x}\lambda^{w}_{i}$. The end-to-end encounter rate constant, k_{en}, also enters the kinetic scheme as the chemical reaction exit pathway. Finally, spin relaxation processes within the electronic manifold must also be considered. To unravel this kinetic scheme with a single experimental technique is not possible. By using several different methods, however, a consistent kinetic picture for the exit channels of the biradicals has evolved and will be developed in the subsequent sections.

Electron Paramagnetic Resonance Experiments

The technique of recording EPR spectra of transient biradicals in liquid solution has been described in detail in previous publications.[2,9] The biradicals are generated inside the cavity of an EPR spectrometer by a 15 ns pulse from an excimer laser using, in most cases, a flow system to avoid sample depletion. The EPR spectrometer operates without field modulation, and the signal from the microwave bridge is passed through a preamplifier into two gated integrators of a boxcar signal averager. The voltage difference between the gates is continuously downloaded to a computer as the external magnetic field is swept to collect the complete EPR spectrum. Most of the spectra reported here were obtained with a laser repetition rate of 80 Hz, gate widths of 150 ns, and a magnetic field sweep of 200 G over a scan time of 4 min. The time resolution of the experiment is limited by the response time of the preamplifier, which is approximately 300 ns in our system. It should be emphasized that the spectra recorded in this way are not the derivative spectra obtained in most EPR experiments, but true absorption and emission spectra.

Figure 1 shows the EPR spectra obtained upon laser photolysis of the α,α,α′,α′-tetramethylated cycloalkanones from C_7 to C_{18} in *n*-octane at −7 °C with the sampling boxcar gate set at 500 ns after the laser pulse. At that time and temperature, the major intermediates present are the acyl–alkyl biradicals, as determined from the simulations discussed below. Figure 2 shows the spectra obtained from the same ketones in octane at 57 °C with the sampling gate set to 1 μs after the laser pulse. As can be seen from inspection, a totally different set of spectra has been recorded, which by simulation are shown to arise from the bisalkyl biradicals generated from their immediate precursors by decarbonylation. At temperatures and gate times intermediate between the two sets shown in the figures, superpositions of acyl–alkyl and bisalkyl biradical spectra were obtained.

As the spectra clearly show, the biradicals of both series are strongly spin polarized, giving rise to enhanced absorption and emission lines. The shorter chains give mostly emissive spectra while the longer ones have alternating enhanced absorption and emission lines. This makes them distinctly different from conventional CIDEP spectra from doublet state radicals which have all emissive (absorptive) lines on the low field half and absorptive (emissive) lines at the high field half of the spectrum.

Model for the Interpretation of the EPR Data. The theory underlying the biradical electron spin polarization has been described in detail in previous papers[9,10] and will not be repeated here. However, it will be useful to sketch a physical picture of the underlying quantum mechanics and dynamics of the model with the help of the energy level diagram shown in Figure 3. This diagram is based on the spin Hamiltonian **H** (eq 1) for a rapidly tumbling biradical in which the anisotropic interactions are averaged out and therefore omitted.

$$\mathbf{H} = \beta_e B_0 \hbar^{-1}(g_1 \mathbf{S}_{1z} + g_2 \mathbf{S}_{2z}) - J(1/2 + 2\mathbf{S}_1 \cdot \mathbf{S}_2) + \sum a_i \mathbf{S}_1 \cdot \mathbf{I}_i + \sum a_j \mathbf{S}_2 \cdot \mathbf{I}_j \quad (1)$$

(7) Turro, N. J. *Modern Molecular Photochemistry*; Benjamin/Cummings: Menlo Park, CA, 1978.
(8) Matsui, K.; Mori, T.; Nozaki, H. *Bull. Chem. Soc. Jpn.* **1971**, *44*, 3440.
(9) Closs, G. L.; Forbes, M. D. E.; Norris, J. R., Jr. *J. Phys. Chem.* **1987**, *91*, 3592.
(10) (a) Closs, G. L.; Forbes, M. D. E. *J. Phys. Chem.* **1991**, *95*, 1924. (b) Closs, G. L.; Forbes, M. D. E. In *Kinetics and Spectroscopy of Carbenes and Biradicals*; Platz, M., Ed.; Plenum: New York, 1990; pp 51–75.

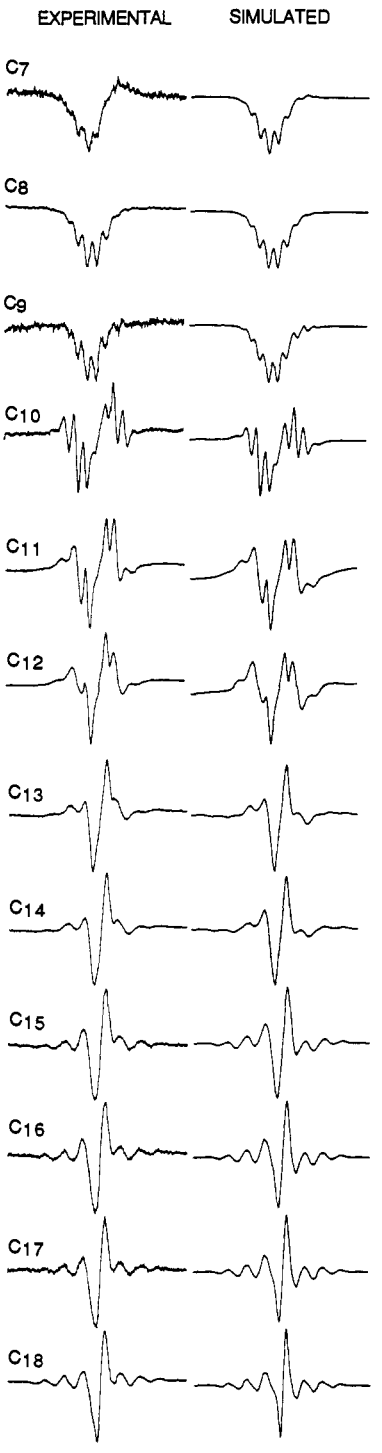

Figure 1. Experimental (left) and simulated (right) direct detection EPR spectra of acyl–alkyl biradicals of the chain lengths indicated, obtained at −7 °C in *n*-octane. In these and all subsequent EPR spectra, the sweep width is 200 G centered at $g = 2$, and lines above the baseline represent enhanced absorption while those below the baseline represent emissive transitions. Kinetic and magnetic parameters used in the simulations are listed in Table I.

The first term in eq 1 is the electronic Zeeman interaction with the indices 1 and 2 referring to the two radical centers of the biradical (β_e is the Bohr magneton, B_0 is the applied magnetic field, and $\hbar$ is Planck's constant divided by 2π). The scalar electron coupling term of magnitude $2J$ is next, followed by the scalar hyperfine interaction terms on both ends of the chain. The nuclear Zeeman term can be omitted because it has no influence on the final EPR spectrum. The basis set is constructed from the direct product of the four electronic spin functions (S, T_+, T_0, and T_-) with all the nuclear functions. For a biradical with n hyperfine

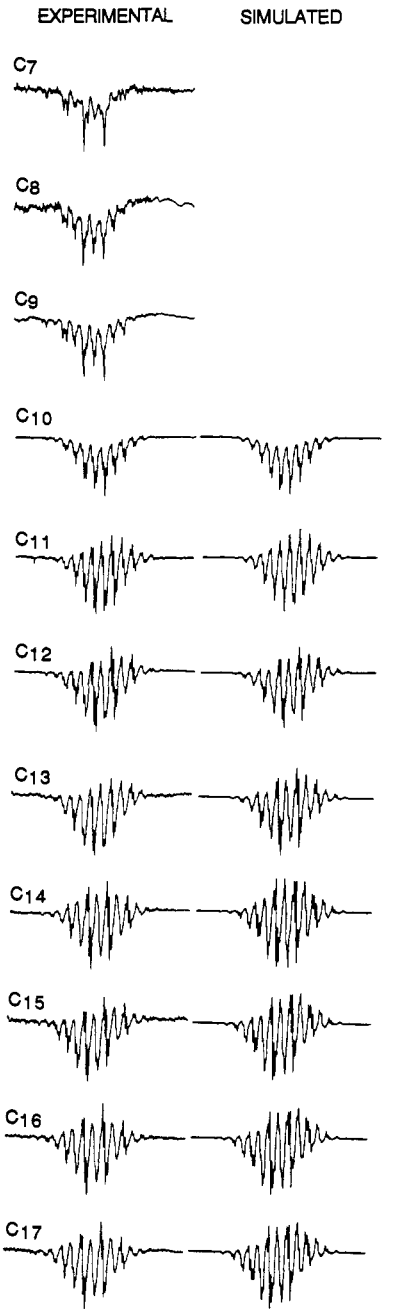

Figure 2. Experimental (left) and simulated (right) direct detection EPR spectra of bisalkyl biradicals of the chain lengths indicated, obtained at 57 °C in *n*-octane. Kinetic and magnetic parameters used in the simulations are listed in Table I.

coupled protons, there are 4×2^n states which translates into 262 144 states for tetramethylated bisalkyl biradicals ($n = 16$).

The left side of Figure 3 shows the levels before hyperfine induced mixing is "turned on". The right side shows the result of the mixing between T_0 and S, pushing the levels apart. It is assumed that for $|2J| < g\beta B_0$, the energy gap between S and T_+ or T_- is too large for effective mixing. A quantitative solution of the stochastic Liouville equation appropriate for this model gives the normalized populations of the four electronic states of the biradical in a hyperfine state defined by nuclear spin quantum numbers m_i and m_j, given by eqs 2 and 3 without considering the

$$\rho_{11} = \frac{1}{3} \tag{2a}$$

$$\rho_{22} = \left(\frac{1}{3}\right)\left(\frac{q^2 \sin^2(\omega t)}{\omega_2}\right) \tag{2b}$$

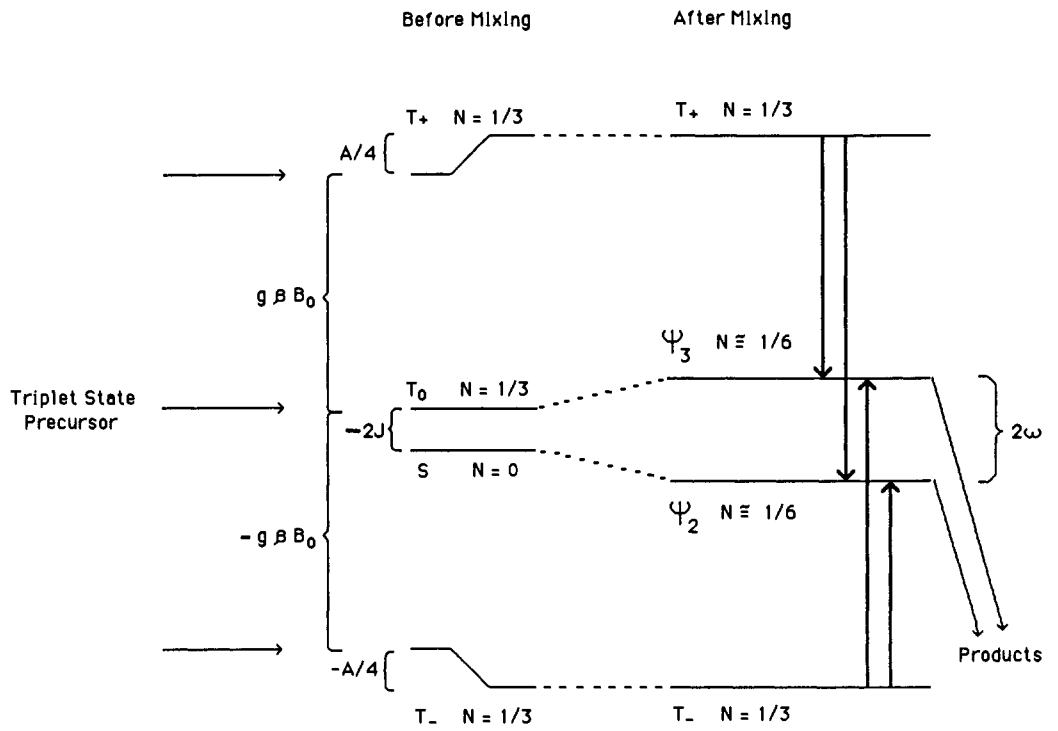

Figure 3. Energy level diagram for a rapidly tumbling biradical in solution.

Table I. Kinetic and Magnetic Parameters Used in Biradical EPR Simulations in Figures 1 and 2

I. Parameters Common to All Simulations

parameter	value	units	ref
a_β, 4 × CH_3	62.2	MHz	12b
a_β, 2 × CH_2	49.8	MHz	12b
g (alkyl)	2.0026		12b
g (acyl)	2.0008		12a
line width (acyl)	8.0	G	*a*
line width (alkyl)	1.8	G	*a*
k_u (uncorrelated dipolar relaxation)	5×10^5	s^{-1}	*a*
$k_{so} + k_{dc}$ (acyl)	5.0×10^6	s^{-1}	*a*
$k_{so} + k_{dc}$ (alkyl)	1.0×10^5	s^{-1}	*a*

II. Parameters Specific for Each Chain Length

chain length and type	$J \pm 5\%$ (MHz)	$k_{en} \pm 50\%$ (s^{-1})	lifetime broadening[b] ±5% (G)	k_{d1}[c] (s^{-1})	k_{d2}[c] (s^{-1})	temp (K)
C_{10} alkyl	−1680	1.0×10^{10}		4.4×10^5	4.9×10^5	330
C_{11} alkyl	−630	1.0×10^{10}		3.0×10^5	3.3×10^5	330
C_{12} alkyl	−560	1.5×10^{10}		2.2×10^5	2.5×10^5	330
C_{13} alkyl	−462	1.5×10^{10}		1.8×10^5	2.0×10^5	330
C_{14} alkyl	−227	1.8×10^{10}		1.5×10^5	1.7×10^5	330
C_{15} alkyl	−224	2.0×10^{10}		1.5×10^5	1.7×10^5	330
C_{16} alkyl	−221	2.0×10^{10}		1.4×10^5	1.6×10^5	330
C_{17} alkyl	−221	2.0×10^{10}		1.4×10^5	1.5×10^5	330
C_7 acyl	−21000	$>1.0 \times 10^{10}$		2.2×10^6	2.5×10^6	266
C_8 acyl	−8400	$>1.0 \times 10^{10}$		9.8×10^5	1.1×10^6	266
C_9 acyl	−2100	$>1.0 \times 10^{10}$		5.4×10^5	6.0×10^5	266
C_{10} acyl	−574	5×10^9	200	3.1×10^5	3.5×10^5	266
C_{11} acyl	−148	1×10^9	37	2.0×10^5	2.3×10^5	266
C_{12} acyl	−101	9×10^8	25	1.4×10^5	1.6×10^5	266
C_{13} acyl	−31	3×10^8	7	1.1×10^5	1.2×10^5	266
C_{14} acyl	−27	3×10^8	6	8.7×10^4	9.8×10^4	266
C_{15} acyl	−20	3×10^8	6	8.1×10^4	9.0×10^4	266
C_{16} acyl	−15	1×10^8	1	7.6×10^4	8.5×10^4	266
C_{17} acyl	−13	1×10^8	1	7.2×10^4	8.0×10^4	266
C_{18} acyl	−8.0	$<1 \times 10^8$	<1	7.0×10^4	7.9×10^4	266

[a] Varied in simulations to best fit. [b] The line width in some simulations must be increased for best fit due to the short lifetime of some of the substates involved in the transitions. The increase is scaled to the sum of the fractions of singlet character of the particular substates. It is a relatively small effect when k_{en} is small, and when k_{en} or J is large the transitions in question are either completely broadened or have low transition probabilities; therefore, this parameter no longer affects the fit. A more complete analysis of this parameter will be presented in a future publication.[20] [c] Calculated from eq 18 of ref 10a.

$$\rho_{33} = \left(\frac{1}{3}\right)\left(1 - \frac{q^2 \sin^2(\omega t)}{\omega^2}\right) \quad (2c)$$

$$\rho_{44} = \frac{1}{3} \quad (2d)$$

$$\omega = (J^2 + q^2)^{1/2} \quad (3a)$$

$$q = \frac{[\beta B_0(g_1 - g_2) + \sum(a_i m_i - a_j m_j)]}{2} \quad (3b)$$

exit channels. The entrance into the acyl–alkyl biradical states is restricted to the triplet manifold because of the pure triplet character of the ketone precursor. The exit to diamagnetic products, however, requires some singlet character and is shown to occur only via the two mixed states, Ψ_2 and Ψ_3, both of which have some singlet character. Assuming no polarization in the precursor ketone, the combined population in both states will be 1/3 with the major fraction being in Ψ_3. In a dynamic situation with a triplet precursor, there actually will be oscillatory behavior of the two states derived from S and T_0, with a frequency ω defined by eq 3a and amplitude of q^2/ω^2, where q is the off-diagonal element between singlet and triplet wave functions defined in eq 3b. Since ω is typically of the order of 10^9 s^{-1} or larger and the observation times are 150 ns or longer, it is permissible to replace the $\sin^2$ functions by their time average of 1/2, yielding

$$\rho_{22} = \left(\frac{1}{3}\right)\left(\frac{q^2}{2\omega^2}\right) \quad (4a)$$

$$\rho_{33} = \left(\frac{1}{3}\right)\left[1 - \frac{q^2}{2\omega^2}\right] \quad (4b)$$

To complete the model it is necessary to consider electron spin relaxation during the biradical lifetime and to include the chemical reaction exit channel from the nuclear substates. Following de Kanter and collaborators,[3] we incorporate two relaxation mechanisms, one based on fluctuations of the dipolar interactions between the two unpaired electrons, and one based on uncorrelated interactions of each electron with the bath. The former mechanism requires two rate constants, k_{d1} and k_{d2}, which represent single and double electron spin flips, respectively, while the latter is described by a rate constant k_u which remains constant throughout the simulations.

It is assumed that the chemical reaction rate constant is proportional to the singlet character, ${}^x\lambda^w_i$, which will be different for each electronic (w) and nuclear state (i). Multiplying this singlet character with the encounter rate constant k_{en} gives the total rate constant for the exit of that particular state to diamagnetic products. As will be discussed below in more detail, mixing between the singlet and triplet manifolds does also occur by nuclear spin independent processes, mostly spin–orbit coupling k_{so}. The model developed so far is adequate for small values of $|J|$. If $|J|$ approaches the same order of magnitude as the Zeeman splitting, it is necessary to include the effect of mixing with T_+ and T_- as well. For negative values of J, mixing of S with T_- will predominate and give rise to more emissive spectra, which are clearly seen in Figures 1 and 2, while positive J values will give enhanced absorption.

It is useful to summarize the kinetic features of the model because it is the basis for understanding all experiments discussed in this paper and because it differs somewhat in the formal description of some of the steps in a model proposed by other investigators.[4] (i) Photoexcitation of the ketone leads to its excited singlet state followed by intersystem crossing to the lowest triplet state on the picosecond time scale. It is assumed that the effects of unequal populations of the ketone triplet state sublevels are small enough to be neglected as are any population differences arising from the Boltzmann distribution. The triplet and singlet states of the ketone are well separated in energy compared to the energy of any coupling terms and can therefore be considered pure spin states. (ii) Thermally activated bond cleavage occurs, taking a few nanoseconds or less for the tetramethylated ketones. This step is nonadiabatic with respect to the electron spins but closes the energy gap between the states derived from the singlet and triplet of the ketone to a few cm^{-1} or less. (iii) The g-factor differences and hyperfine interactions cause mixing to yield a coherent superposition of the four states. With a nonzero J, the triplet-derived states acquire some small degree of singlet character, and the singlet-derived state has the equivalent amount of triplet character. All three triplet sublevels are mixed with the singlet, but the one closest in energy to the singlet is most affected. Initially, there are distinct oscillations with different frequencies and amplitudes for every nondegenerate nuclear sublevel. The coherence of the electron spin states is lost with T_2 of the acyl–alkyl biradicals, which in the compounds studied is less than 100 ns as estimated from the EPR line widths. (iv) Decarbonylation of the acyl–alkyl biradicals is treated as an electron and nuclear spin independent process, thus conserving both spin angular momenta. The initial spin state distributions of the bisalkyl biradicals is therefore set as the one obtained from the precursor acyl–alkyl biradicals. (v) Relaxation transitions among all four states can become the major mechanism leading to diamagnetic products. (vi) Reaction to diamagnetic products occurs from all states with rates proportional to the singlet character of that state. In the absence of relaxation there are no transitions between the electronic states. *It is therefore misleading to talk about an intersystem crossing step in the biradical and assign it a rate constant. Only in systems with extremely small or vanishing J where the amplitudes reach from pure triplet to almost pure singlet character and the reaction occurs within the first one or two oscillations, as can be the case in radical pairs, has that picture any meaning.*[11]

Interpretation and Discussion of the EPR Data. The model just outlined forms the basis for a computer simulation program as described in a previous paper.[10a] The g factors and hyperfine coupling constants used in the simulations are taken from the literature for equivalent monoradicals.[12] The kinetic parameters discussed above and the J values are adjusted to produce the best fit to the experimental spectra. The simulations are shown on the right-hand sides of Figures 1 and 2, which made use of the parameters listed in Table I. In general, the simulations must be considered satisfactory with the exception of the first three short chain members of the bisalkyl biradicals. These three spectra were obtained under slightly different conditions from the others. Owing to the small amount of material obtained in the synthesis of the precursors, the EPR spectra for these biradicals were obtained by photolysis at high temperatures of single 4 mm o.d. quartz sample tubes at very high concentrations (≥0.5 M). At these high concentrations and temperatures, both intra- and intermolecular dipolar relaxation mechanisms may be dominating the kinetics. Repeated attempts to simulate this effect were unsuccessful, and there may well be some other mechanism responsible for the shape of these spectra.

The first interesting result derived from the simulations is that in all compounds J is negative, or that the biradicals have singlet ground states. This is in line with expectations for long chain biradicals as pointed out by Dougherty.[13] If the triplet had been the ground state, the spectra would have the appearance obtained after a 180° rotation around the base-line axis. If the signs of the hyperfine interactions are known, this determination of the spin multiplicity of the ground state of biradicals is totally unambiguous. The usual experimental method used to extract this information is to construct a Curie plot, a difficult procedure not always free of misinterpretation.

The next valuable information obtainable from the simulations is the magnitude of J, or the singlet–triplet splitting, and its

(11) This approach, developed in our laboratory, has recently been accepted by other researchers, e.g.: Evans, C. H.; Scaiano, J. C. *J. Am. Chem. Soc.* **1990**, *112*, 2649.

(12) (a) Schuh, H.; Hamilton, E. J., Jr.; Paul, H.; Fischer, H. *Helv. Chim. Acta* **1974**, *57*, 2011. (b) Ohno, N.; Kito, N.; Ohnishi, Y. *Bull. Chem. Soc. Jpn.* **1971**, *44*, 470.

(13) Dougherty, D. A.; Goldberg, A. H. *J. Am. Chem. Soc.* **1983**, *105*, 284.

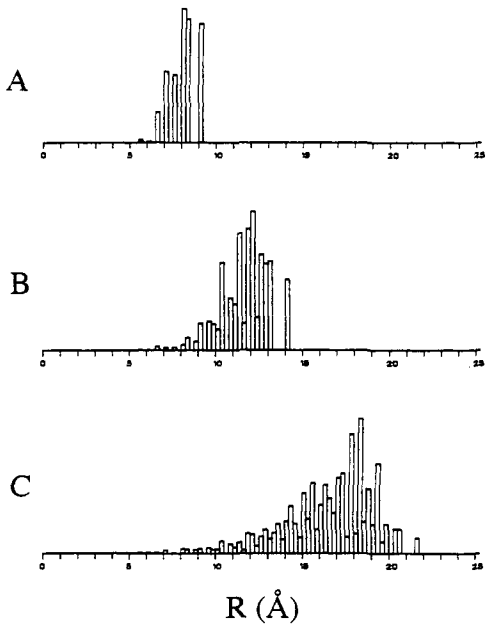

Figure 4. Unnormalized histograms of end-to-end distance for *n*-alkane chains from the Monte Carlo program of ref 14. A total of 5×10^5 samples were taken for each of the three chain lengths: (A) 8 carbon atoms, (B) 12 carbon atoms, (C) 18 carbon atoms.

dependence on chain length. To analyze the chain length dependence it must be pointed out that the J value, as it determines the spectral appearance, is a time-averaged value over all the conformations visited by the polymethylene chain, much as is the J coupling constant in NMR spectra of a rotating methyl group with a vicinal proton. The fact that relatively sharp lines are discernible in the spectra of the bisalkyl biradicals is an indication that the averaging does indeed take place within the time scale of the inverse of the line width (100 ns). Therefore, with a jump time of 30 ps between conformations,[14] a conformational equilibrium can definitely be assumed for the shorter chain lengths. In fact, this assumption works well for all of the chain lengths studied here.

To elucidate the mechanism of the J coupling, it is necessary to choose a model for the chain length dependence. The most common through-space model assumes an exponential dependence of the coupling on distance as shown in eq 5, where R is the

$$J = J_0 \exp[-\beta(R - R_0)] \quad (5)$$

end-to-end distance and R_0 is the reaction radius defined as the distance where the attractive potential in the singlet state becomes comparable to k_BT, where k_B is Boltzmann's constant and T is the absolute temperature. To calculate an average J value for such a mechanism, a distribution function of end-to-end distances for each biradical chain length is required. For simplicity we have adopted the method of Nairn and Braun[14] which is based on Flory's rotational isomeric state model.[15] This procedure puts the polymethylene chain into a diamond lattice and constructs the conformations by assigning each four-carbon fragment in the chain one of three dihedral angles: trans coplanar, plus gauche, or minus gauche. Certain combinations of these conformations are excluded because they lead to unnatural crowding. By assigning the trans conformation an energy of 0 and the gauche conformations a value of 0.91 kcal/mol,[16] it is possible to compute an energy for each of the many accessible conformations and obtain an end-to-end distance for them. The distribution is given by the Boltzmann law and the conformations are sampled by Monte Carlo methods. The result, consisting of several hundred thousand samples, is then constructed into a histogram plotting probability versus end-to-end distance in segments of 0.25 Å. Distances smaller than R_0 (3.55 Å) are excluded. Histograms for several chain lengths are shown in Figure 4. It is now possible to construct average J values, $\langle J \rangle$, for any value of β and J_0 by calculating J for any segment of the histogram weighted by its probability. Since J_0 just scales the data set, the major parameter to be adjusted is β, which determines the form of the function of $\langle J \rangle$ with chain length. The deficiency of this model lies in its neglect of excluded volume in some conformations, weighing the shorter distances too heavily. However, the influence of this error on β is estimated to be small.[17]

Electron spins can also be coupled through the σ-bonds of the biradicals. There is ample evidence that electronic interactions through the σ-framework follow an exponential attenuation with the number of bonds, N, leading to the expression[18]

$$J = J_0' \exp[-\gamma(N - 1)] \quad (6)$$

Here, J_0' is the coupling between two electrons separated by one σ-bond. A different averaging procedure is used to calculate the through-bond J averaged over all possible conformations. The statistical parameter required is the number of gauche bonds, as this is the most direct way to measure the decrease in the through-bond coupling as the chain assumes the more "coiled up" conformations. The same Monte Carlo computer program is used to generate histograms of the number of gauche bonds for each chain length. Semiempirical molecular orbital calculations (MINDO/3) on a model system, 1,8-octanediyl, are then used to assign each box in the histogram a coefficient which reflects the decrease in the J coupling for that number of gauche bonds. It is worth noting that the through-bond model predicts the maximum coupling for the all-trans conformation,[19] in direct contrast to the through-space mechanism which predicts the smallest coupling because it corresponds to the longest distance. Also, the more gauche conformations included in the chain, the steeper the distance dependence of the through-bond mechanism.[10b]

Attempts to fit the experimental data points obtained for the acyl–alkyl biradicals exclusively to either the through-space or the through-bond model failed. The shorter chains, C_7 through C_{12}, show the expected exponential falloff for the through-bond model, but the longer ones show a less drastic dependence on the number of carbon atoms. The through-space model fails to cover the experimentally observed range with any reasonable value of β. One possible solution to the problem is that a mixed mechanism is at work with through-bond coupling dominating for the shorter chains and the through-space coupling for the longer ones. While the data can be fit to such a combination, it cannot be considered proof. It is certainly reasonable that the through-bond mechanism will become negligible with a large number of σ-bonds, leaving the through-space mechanism the only contributing factor. Figure 5A shows the best fit to a linear combination of the two mechanisms. Possible evidence for the mixed mechanism can be obtained from the temperature dependence of the average J values. The end-to-end distribution function changes predictably with temperature, favoring the longer distances at lower temperature. Therefore, a through-space mechanism should have a positive temperature coefficient while the through-bond one is expected to be negative. Preliminary data support this prediction.[20] Further tests of this prediction over a larger temperature range are the subject of research in progress. The chain length dependence in the bisalkyl biradicals shows behavior similar to the acyl–alkyl series, with a leveling off at longer chain lengths. The leveling occurs at a higher value compared to acyl–alkyl biradicals. Part, if not all, of this can be attributed to the positive temperature coefficient expected for the longer chains and the fact that the bisalkyl biradical spectra were recorded at significantly higher

(14) Nairn, J. A.; Braun, C. L. *J. Chem. Phys.* **1981**, *74*, 2441.
(15) Flory, P. J. *Statistical Mechanics of Chain Molecules*; Wiley: New York, 1969.
(16) Taken from an MM2 calculation on *n*-butane.
(17) Freed, K. F. Private communication.
(18) (a) McConnell, H. M. *J. Chem. Phys.* **1961**, *35*, 508. (b) Closs, G. L.; Miller, J. R. *Science* **1988**, *240*, 440.
(19) Beratan, D. N.; Onuchic, J. N. *J. Am. Chem. Soc.* **1987**, *109*, 6771.
(20) Closs, G. L.; Calle, P.; Gautam, P.; Forbes, M. D. E. To be published.

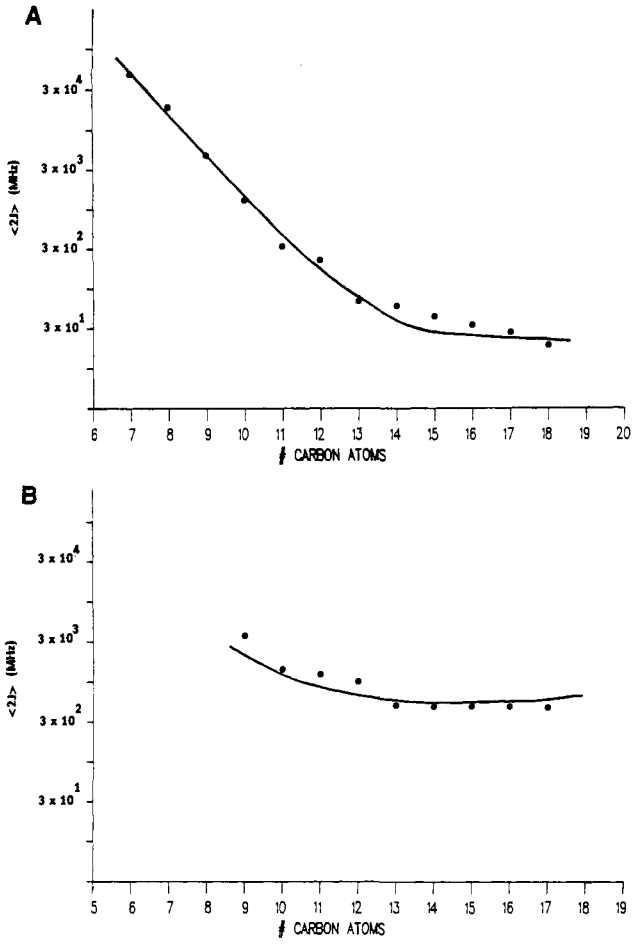

Figure 5. Best fit (solid line) to the experimental chain length dependence (solid dots) of a sum of the through-bond and through-space mechanisms for electronic spin–spin coupling. The fitting function was $J = A \exp[-\gamma(N-1)] + B \exp[-\beta(R-R_0)]$: (A) acyl–alkyl biradicals at −7 °C, with $A = 4.0 \times 10^{13}$ s^{-1}, $B = 5.5 \times 10^{11}$ s^{-1}, $\beta = 1.06$ Å^{-1}, $\gamma = 1.15$/C atom. (B) bisalkyl biradicals at 57 °C, with $A = 1.0 \times 10^{11}$ s^{-1}, $B = 2.0 \times 10^{12}$ s^{-1}, $\beta = 1.06$ Å^{-1}, $\gamma = 1.15$/C atom.

temperature. Figure 5B shows the best fit to a model based on the mixed through-bond and through-space mechanism. As is the case for the acyl-alkyl series, this fit is probably not a unique solution.

Since the EPR spectra are taken in a time-resolved mode, it should be possible to obtain reaction kinetics from the data. The decay of the signals with time is a complicated function because of the many processes contributing to it. A detailed analysis for the time dependence of the signals obtained for several biradicals has been given in the previous paper[10a] and will not be repeated here except for summarizing the results. First, each nuclear spin state, or set of degenerate states, decays with a different rate constant. Only in cases in which nuclear spin independent processes such as spin–orbit coupling are very predominant as in the acyl–alkyl biradicals can one expect an approximate exponential decay. This important conclusion is supported by the change in the shape of the bisalkyl biradical spectrum with time,[10a] and by the previously reported time dependence of the CIDNP spectra of the products.[21] As a consequence of the different time dependence of individual hyperfine lines, it is necessary to simulate the entire spectrum at separate delay times to extract any kinetic parameters of value.

Among the adjustable parameters in the simulations is k_{en}, whose product with ${}^{x}\lambda^{w}_{i}$, the singlet character of the individual electronic and nuclear substates, gives the rate constant for that state for product formation. Nuclear substate independent channels are described by the sum of ${}^{ac}k_{so}$ and k_{dc} for the acyl–alkyl biradicals and ${}^{al}k_{so}$ for the bisalkyl biradicals. Finally, the dipolar interaction-induced relaxation rates k_{d1} and k_{d2} are calculated from the end-to-end distance histograms using the appropriate averaging function given by de Kanter et al.[3,10a] For the uncorrelated relaxation rates a single parameter is adjusted to give values appropriate for monoradicals (≈ 2 μs) and held constant throughout the series.

The following general conclusions can be drawn from the simulations. (i) They are not very sensitive to the encounter rate constant k_{en}, yielding an uncertainty of 50% from the best value. For the acyl–alkyl biradicals, k_{en} varies with chain length from 10^{10} to 10^{8} s^{-1} as listed in Table I. (ii) Nuclear spin independent exit channels predominate in the product formation steps in the acyl–alkyl biradicals, with the sum of ${}^{ac}k_{so}$ and k_{dc} equal to 5×10^{6} s^{-1}. In the bisalkyl biradicals, ${}^{al}k_{so}$ is much smaller, in the range of 10^{5} s^{-1} or less. (iii) Electron spin relaxation is relatively unimportant in the acyl–alkyl biradicals, but is probably the major factor in the disappearance of the bisalkyl spectra.

The EPR studies on both acyl–alkyl and bisalkyl biradicals are useful for determining the average exchange coupling $\langle J \rangle$. This, together with the known hyperfine coupling constants and g-factor differences, gives an accurate estimate of the degree of singlet–triplet mixing in the four electronic states. The EPR experiments are also quite informative in explaining why the biradicals can have lifetimes in the microsecond range with encounter rates in excess of 10^{9} s^{-1}. This is due to the fact that poor state mixing gives the initially populated levels little singlet character, requiring many thousands of end-to-end encounters before chemical reaction takes place. For very small J, the T_0 level depletes rapidly but T_+ and T_- have to wait for a relaxation transition before they can react. For larger J, as a result of the Zeeman splitting, T_- depletes more rapidly as evidenced by the predominantly emissive character of the spectra, but T_0 and T_+ are then dependent on relaxation.

It is interesting to note that the presence of an acyl radical site on the biradicals increases the spin–orbit coupling rate by over two orders of magnitude. At the same time, the EPR line widths are also increased substantially by the acyl group.[22] It is tempting to speculate that the two phenomena are related. If the bent σ-state of the acyl group mixes with the linear π-state, spin–orbit coupling could be greatly increased, leading both to a short T_2 and a fast intersystem crossing. The large energy gap between the σ- and π-state (~ 1 eV)[23] assures that this mixing is small, but it may still have a significant effect. The known positive temperature dependence[22] of the line width of acyl radicals supports this mechanism.

The deficiencies of the EPR experiments are (i) its poor time response, which leads to inaccurate decay kinetics for the short lived acyl–alkyl biradicals, and (ii) its inability to separate the relative importance of the two nuclear-spin independent rate processes, decarbonylation and spin–orbit coupling. Other techniques are clearly necessary to answer these questions, and this was the motivation for initiating the transient optical absorption and magnetic field effect experiments described below. Additionally, the EPR experiments are not the only technique by which the average J coupling can be measured. In principle, intensity maxima obtained from variable magnetic field CIDNP experiments can yield average J values, and it is to this experiment we now turn for a comparison to the EPR data.

Variable Magnetic Field CIDNP Experiments

The original study of the field dependence of the CIDNP intensities of biradical products was performed on a similar series of ketones, except that they were not alkylated at the α-positions and, therefore, the biradicals did not decarbonylate during their lifetimes.[1] To make this study more complete, we have investigated five methylated cyclic ketones and remeasured two unsubstituted compounds as a reference, all of which are shown in Table II. The samples were dissolved in $CDCl_3$ and degassed by bubbling dry

(21) Closs, G. L.; Redwine, O. D. *J. Am. Chem. Soc.* **1985**, *107*, 6131.

(22) Paul, H. *Chem. Phys. Lett.* **1975**, *32*, 472.

(23) Austin, J. A.; Levy, D. H.; Gottlieb, C. A.; Redford, H. E. *J. Chem. Phys.* **1974**, *60*, 207.

Table II. Variable Magnetic Field CIDNP Result for Acyl–Alkyl Biradicals

compound	B_{max}^{CIDNP} (MHz)	$2J^{EPR}$ (MHz)
cyclooctanone	11 600 ± 10%	
dimethylcyclooctanone	11 800 ± 10%	
tetramethylcyclooctanone	6 700 ± 10%	−16 800
tetramethylcyclodecanone	1 700 ± 10%	−1 150
cyclododecanone	420 ± 20%	
tetramethylcyclododecanone	500 ± 20%	−202
tetramethylcyclopentadecanone	200 ± 30%	−40

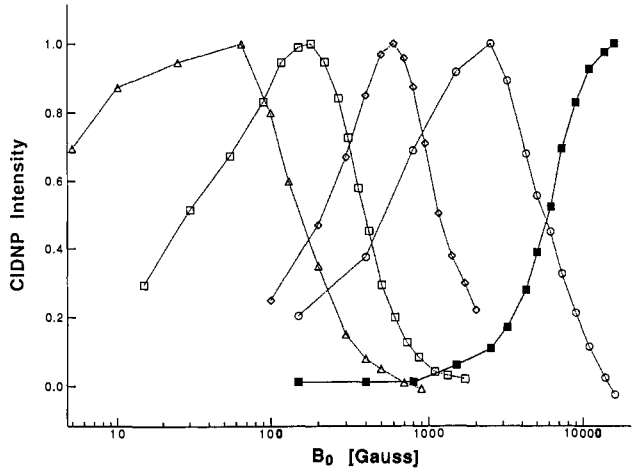

Figure 6. Variable field CIDNP results: The aldehyde peak intensity plotted against applied external magnetic field for: △, tetramethylcyclopentadecanone; □, tetramethylcyclododecanone; ◇, tetramethylcyclodecanone; and ○, tetramethylcyclooctanone. The symbol ■ represents the intensity of the vinylic methyl group peak corresponding to the disproportionation product of the bisalkyl biradical formed by decarbonylation after photolysis of tetramethylcyclooctanone.

nitrogen through them. A circulation system was used with a flow rate of 0.1 to 0.2 mL/s. The sample was photolyzed in the gap of an auxiliary variable field electromagnet (0 to 1.8 T) and subsequently pumped into a specially designed, home-built flow probe of a 60 MHz Bruker WP-60 FT NMR spectrometer. Pseudo-CW excitation with an excimer laser running at 100 Hz repetition rate was employed. The intensity of the aldehyde peak in the product's NMR spectrum was monitored as a function of the field. The variable magnetic field CIDNP measurements required relatively large quantities of starting ketone. Even with the unusually small diameter of the flow probe used in this study (i.d. of 1.99 mm), at least 2 g of ketone was required for each experiment.

Figure 6 shows the field dependence of the intensity of the aldehyde signal of the major disproportionation product for the tetramethylated cycloalkanones. The most rudimentary interpretation of the field dependence of the CIDNP signals equates the field position at which the signal is maximized, B_{max}, with the average magnitude of $|2J|$. This follows from the notion that the most efficient S to T_- mixing should occur in the crossing region between the two states. Table II shows the comparison of the $|\langle 2J\rangle|$ values obtained from the EPR and CIDNP measurements. The agreement is poor, with the ratio of the two values varying by more than an order of magnitude over the seven carbon atom range of chain length. A more refined analysis of the older CIDNP data on unmethylated ketones by de Kanter and collaborators[3] has already pointed out the fact that the maximum CIDNP intensities, while related to the average exchange coupling, are not expected to occur at exactly $B_{max} = |2J|$.

The conclusion to be drawn from this comparison is that a simplistic evaluation of the field dependence of CIDNP intensities gives poor results for the exchange coupling unless a complete solution of the stochastic Liouville equation is obtainable. Unfortunately, at the present time this is impossible for systems containing as many spin states as the molecules investigated in this study, and we can offer only the following qualitative explanation of the above discrepancy: as opposed to EPR, which does indeed measure the J averaged over the observation time (the width of the boxcar gate), CIDNP gives values that are weighted toward the chain conformations and end-to-end distances suitable for the formation of products. This notion is supported by the results for the longer chain lengths from C_{10} to C_{15}, for which the B_{max} value obtained from the CIDNP measurements is consistently larger than the corresponding $|2J|$ value from the EPR fits. The ratio of these values increases with the increasing chain length, as one would expect it to do, since the longer the chain, the larger the difference between the average end-to-end distance and the reaction radius. Even more significantly, this trend parallels the temperature dependence of J established by EPR (see the discussion above). We cannot, however, account in the same manner for the very low B_{max} for tetramethylcyclooctanone, or for the dramatic difference between this ketone and its dimethylated and unmethylated analogues.

Table III. Decay Rates of Acyl–Alkyl Biradicals at Zero Magnetic Field

compound	k (s^{-1})
tetramethylcyclooctanone	1.4×10^7 ± 20%
tetramethylcyclododecanone	1.5×10^7 ± 20%
tetramethylcyclotridecanone	1.5×10^7 ± 20%
tetramethylcyclotetradecanone	1.5×10^7 ± 30%
2-adamantanone	6.7×10^7 ± 30%
bicyclo[3.3.1]nonan-9-one	4.6×10^7 ± 30%

Nevertheless, tetramethylcyclooctanone did yield a very interesting, if unexpected, result. It was the only tetramethylated ketone for which it was possible to resolve a CIDNP signal corresponding to the diamagnetic products of the bisalkyl biradical resulting from decarbonylation of its acyl–alkyl precursor. The magnetic field dependence of the vinylic methyl peak was obtained (Figure 6). Its shape, with $B_{max} \geq 15\,000$ G, is characteristic of a seven-membered biradical.[1,3] To our knowledge this is the first CIDNP observation of products from a bisalkyl biradical.

Transient Optical Absorption Experiments

To obtain information on the overall kinetics of the reactions discussed above, a transient optical absorption study was initiated. A typical setup with an excimer laser (308 nm) serving as the excitation source was used. For the variable magnetic field measurements, the sample cell holder was placed in the gap of a 12 in. Harvey–Wells electromagnet. One difficulty associated with this work arises from the rather poor absorption characteristics of the biradicals under investigation. The aliphatic acyl group has been reported to have an absorption maximum at 220 nm of medium extinction coefficient with a rather long tail toward longer wavelengths.[24] The alkyl radicals absorb in this region also, with extinction coefficients about one-third that of the acyl radicals. Therefore, the sensitivity of the experiment is not optimal. Additional problems include solvent absorbance at 220 nm and the absorbance of photoproducts upon prolonged photolysis. Despite this unfavorable situation, it was possible to determine the kinetics of the disappearance of the acyl–alkyl biradicals with reasonable accuracy at 230 nm. Table III lists the data obtained on the lifetimes for some of the biradicals included in the EPR study as well as two biradicals containing a carbocyclic ring. No kinetic information was obtainable from these data for the bisalkyl biradicals.

In spite of the fact that the hyperfine and g factor induced mixing should lead to a nonexponential decay, all the data were satisfactorily fitted with a single decay rate constant. As shown below, this is mostly attributable to the predominance of the spin–orbit-induced intersystem crossing which is in first approximation independent of the spin states. The lifetimes of approximately 70 ns found for the medium-chain acyl–alkyl biradicals are not exceptional and compare well with literature values

(24) Parkes, D. A.; Quinn, C. P. J. Chem. Soc., Faraday Trans. 1 1976, 72(9), 1952.

Table IV. Values of the Singlet–Triplet Splitting $2J$ for Alkyl–Acyl Biradicals Obtained from the Magnetic Field Effect Measurements (MFE) and from the EPR Data

compound	k_{max}/k_0[a]	$2J^{MFE}$ (MHz)	$2J^{EPR}$ (MHz)
tetramethylcyclooctanone	1.05 ± 20%		−16 800
tetramethylcyclododecanone	1.28 ± 20%	−140 ± 20%	−202
tetramethylcyclotridecanone	1.29 ± 20%	−84 ± 20%	−62

[a] The ratio of the maximum decay rate to the decay rate at a zero field.

reported for similar species.[25] The disappearance rates of cyclic biradicals are markedly faster.

Since there are two nuclear spin and g-factor independent exit channels for the biradicals, spin–orbit coupling and decarbonylation, it is of interest to determine which one predominates. Neither the EPR nor the optical data give a direct answer to that question. However, if one assumes that the small coupling between the two radical sites has negligible influence on the spin independent processes, a kinetic investigation of a comparable monoradical should give some information regarding these rates. Consequently, the decarbonylation rate of the pivaloyl radical, generated from the laser flash photolysis of 2,2,4,4-tetramethyl-3-pentanone in hexane, was investigated. The experiment once again is complicated by the low extinction coefficient of the acyl chromophore and the nonnegligible absorption of the *tert*-butyl radical at the wavelength chosen (230 nm) for the measurements. Nevertheless, the signal-to-noise was found to be acceptable. The value determined for the decarbonylation rate constant at 296 K was $1.5 \pm 0.5 \times 10^6$ s^{-1}, which is in line with the lower limit of 10^5 s^{-1} established by Fischer and co-workers.[26] These experiments have provided a relatively accurate rate constant for the total disappearance of the acyl–alkyl biradicals, and the value deduced from the simulations of the EPR measurements, the sum of k_{dc} and $^{ac}k_{so} = 5.0 \times 10^6$ s^{-1}, is consistent with the optically measured value.

From these data, two conclusions can be drawn. First, the major exit channel for the acyl–alkyl biradicals is by intramolecular cyclization and disproportionation because the overall disappearance rate of the biradical is 7 to 15 times faster than the decarbonylation. Second, the chemically induced spin polarization of the bisalkyl biradicals must be extremely large because their concentrations are only a very small fraction of the original concentration of the acyl–alkyl biradicals. The fact that comparable signal intensities are observed can be explained by the larger line width of the acyl–alkyl species (8 to 10 G) versus the bisalkyl line width of 1.8 G.

Magnetic Field Effects on Lifetimes of Acyl–Alkyl Biradicals

Magnetic field effects on the kinetics of radical pair reactions are now well established.[27] They are based on the concept of modifying the mixing that occurs at zero field or low field between the singlet state and the three degenerate levels of the triplet state of a radical pair by introducing a Zeeman splitting between the T_0 state and the T_+ and T_- states, breaking this degeneracy. In biradicals, level crossing between the S state and the T_- state for negative J and the T_+ state for a positive J will yield maxima of the magnetic field effects in the vicinity of magnetic fields that are comparable to the average J coupling. It is generally assumed that intersystem crossing caused by spin–orbit coupling will be quite insensitive to these effects.[27] It is therefore possible to use the magnitude of magnetic field effects to estimate the relative importance of spin–orbit versus hyperfine and g-factor-induced mixing between singlet and triplet states. It is noteworthy that

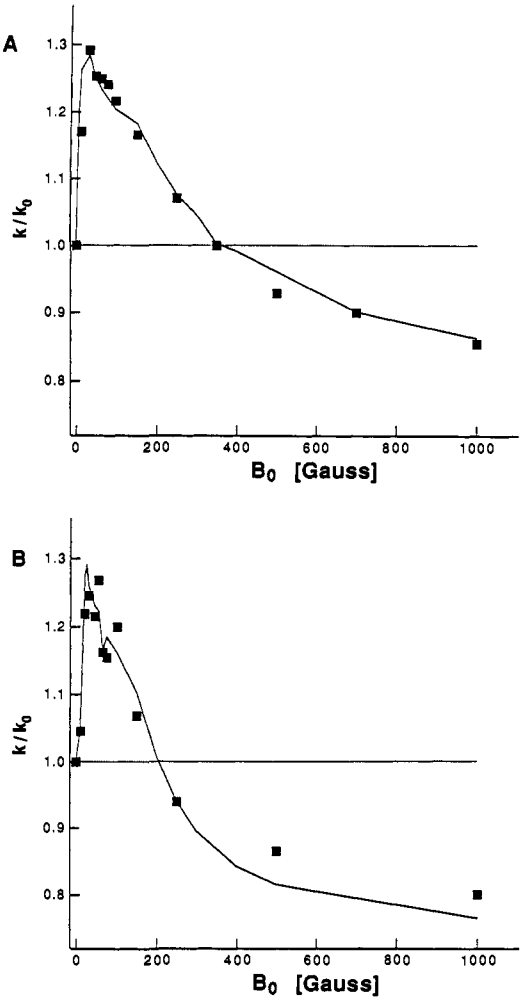

Figure 7. Experimental (■) and calculated (—) magnetic field effects on the decay rate of acyl–alkyl biradicals: (A) tetramethylcyclododecanone and (B) tetramethylcyclotridecanone.

long chain biradicals are predicted to have a larger contribution by the latter mechanism, and therefore a larger magnetic field effect because the large average J in the shorter chains prevents effective mixing by the small difference in the magnetic parameters.

Having determined the magnitude of J by the EPR experiments discussed above, it should be possible to model the magnetic field effects with only one additional parameter, $^{ac}k_{so}$. Table IV shows the results of the magnetic field dependence study for three of the acyl–alkyl biradicals. The tetramethylated C_8 chain shows only a very small magnetic field effect with a maximum increase of 5% in the magnetic field compared to zero field. The expected maximum of the rate in the vicinity of 6000 G could not be discerned with any certainty. However, a very clear magnetic field effect was observed for the C_{12} and C_{13} chains as shown in Figure 7. In each case the rate increases steeply by about 30%, goes through a maximum, and then becomes less than at zero field. A small modification to the computer program developed for the EPR simulations made it possible to simulate the expected field dependence for these biradicals, with the results shown in Figure 7. Specifically, the simulation program reported the projected singlet character for each nuclear sublevel, the sum of which gave the yield of product at each magnetic field for a given chain length. It is worth pointing out that the simulated field dependence is not smooth. Apparently, individual hyperfine sublevels achieve a maximum intersystem crossing rate at different magnetic field values, the effect of which is not completely averaged by the line width of 10 G used in these calculations. Table IV shows the comparison of the J values obtained from the best fits of the EPR data and the optical data. Considering the experimental uncer-

(25) (a) Scaiano, J. C. *Acc. Chem. Res.* **1982**, *15*, 252. (b) Weir, D.; Scaiano, J. C. *Chem. Phys. Lett.* **1985**, *118*, 526.
(26) (a) Fischer, H. *Chem. Phys. Lett.* **1983**, *100*, 255. (b) Schuh, H.; Hamilton, E. J., Jr.; Paul, H.; Fischer, H. *Helv. Chim. Acta* **1974**, *57*, 2011.
(27) Salikhov, K. M.; Molin, Yu. N.; Sagdeev, R. Z.; Buchachenko, A. L. *Magnetic and Spin Effects in Chemical Reactions*; Elsevier: Amsterdam, 1984.

tainty in either method, and keeping in mind that the two methods are based on different phenomena, the discrepancy of 35% in the two results is remarkably small. In addition to J, the magnetic field studies give values for $^{ac}k_{so}$. The best value of 1.2×10^7 s^{-1} is not much different from the one used in the EPR simulations which, as pointed out above, are not very sensitive to this value. The extrapolated lifetimes for these biradicals are in general agreement with those obtained from other methods.[25] The computations also contain a number for k_{en}, listed in Table IV, which is close to the values used in the EPR simulations.

The separation of $^{ac}k_{so}$ from spin-dependent processes has therefore been achieved by the magnetic field dependent flash photolysis. The extremely small field effect observed for the C_8 acyl-alkyl biradicals shows that $^{ac}k_{so}$ predominates over spin-dependent processes for shorter chain lengths. However, the longer chain lengths show substantial field effects. If $^{ac}k_{so}$ is assumed to be independent of chain length, then this must be attributed to better singlet-triplet mixing due to a diminished J value. On the other hand, it is not clear that $^{ac}k_{so}$ is indeed independent of chain length, and the observed trend may well be due to variations in both mechanisms.

Summary

In conclusion it can be stated that a consistent picture has been developed for the kinetics of polymethylene biradicals, which are strongly dependent on both spin and chain dynamics. To unravel the importance of the various exit channels, it was found necessary to employ a broad spectrum of experimental techniques coupled with extensive computations. Theory had matched experiment quite well in most cases, and where it does not there are reasonable explanations. Much has been learned in this work regarding the mechanism of the spin-spin coupling in flexible biradicals and its overall role in the kinetics. Further work is necessary in order to fully understand the temperature dependence of the couplings by either through-bond or through-space mechanisms, and this is now an active part of our research program.

Acknowledgment. The authors thank J. A. Nairn and C. L. Braun for kindly supplying a copy of their Monte Carlo simulation program. M.D.E.F. thanks J. R. Norris for many helpful discussions on the theory of chemically induced electron spin polarization. The support of the National Science Foundation throughout the course of this work is gratefully acknowledged.

A Molecular Merry-Go-Round: Motion of the Large Macrocyclic Molecule 18-Crown-6 in Its Solid Complexes Studied by ^{2}H NMR†

C. I. Ratcliffe,*,‡ J. A. Ripmeester,‡ G. W. Buchanan,§ and J. K. Denike§

Contribution from the Steacie Institute for Molecular Sciences, National Research Council of Canada, Ottawa, Ontario, Canada K1A 0R9, and Ottawa-Carleton Chemistry Institute, Carleton University, Ottawa, Ontario, Canada K1S 5B6. *Received October 7, 1991*

Abstract: ^{2}H NMR line shape measurements were used to confirm and refine a model to account for large-amplitude motions in solid 18-crown-6 complexes previously identified from ^{13}C and ^{1}H NMR results. Reminiscent of the motion of a merry-go-round, the motion is a combined rotation and conformational adjustment of the macrocycle, in which individual $-OCH_2CH_2-$ units jump to adjacent sites in the crystal. Specifically, for the malononitrile complex, 18-crown-6·$2CH_2(CN)_2$, jump rates were obtained by modeling the intermediate-rate line shapes, yielding an activation energy of 47.6 ± 0.8 kJ/mol. Because the motion does not introduce disorder, it is diffraction invisible.

Introduction

Complexes of crown ethers and their derivatives are widely recognized as model systems for molecular recognition. The conformation of the crowns can adapt for optimum complexation of the guest. 18-Crown-6 is the archetypal macrocyclic ether, and calculations on the isolated molecule show that it is very flexible with a large number of possible conformations having only slightly different energies.[1-3] In solution the molecule rapidly interchanges among many conformations,[4] and only a single ^{13}C or ^{1}H NMR signal is observed down to 143 K.[5] In solid 18-crown-6 and its complexes, however, the molecule is usually locked into one of just a few conformations. In the ideal case where all bond angles in the crown are taken as tetrahedral, the C atoms and C-H bonds can be placed on a "diamond lattice",[1] Figure 1. The most stable conformation has D_{3d} symmetry, and the next most stable has C_i. We will refer to the latter as C_i' since many of the other conformations also have C_i symmetry. Both D_{3d} and C_i' are commonly found in solid complexes, though of course in the real world there are usually deviations from tetrahedral angles and the strict symmetry, so that only a pseudo-D_{3d} conformation is observed.

In our recent studies of the ^{13}C cross-polarization/magic angle spinning (CP/MAS) NMR of a number of molecular complexes of 18-crown-6, we found evidence that the macrocycle undergoes some kind of large-amplitude motion in the neighborhood of room temperature;[6-8] namely, (a) the coalescence of any multiple-line structure in the ^{13}C CP/MAS crown ether resonance and (b) the observation that the ^{13}C CP/MAS signal from the crown ether went through a fade-out region over a range of temperatures specific to each complex. The fade-out occurs because of interference between the coherent averaging of the ^{1}H decoupling field and the incoherent averaging due to motion of the molecule.[9] This motion was also confirmed by the narrowing of ^{1}H NMR line

† NRCC No. 33277.
‡ National Research Council of Canada.
§ Carleton University.

(1) Uiterwijk, J. W. H. M.; Harkema, S.; van de Waal, B. W.; Gobel, F.; Nibbeling, H. T. M. *J. Chem. Soc., Perkin Trans. 2* **1983**, 1843.
(2) Uiterwijk, J. W. H. M.; Harkema, S.; Feil, D. *J. Chem. Soc., Perkin Trans. 2* **1987**, 721.
(3) Billeter, M.; Howard, A. E.; Kuntz, I. D.; Kollman, P. A. *J. Am. Chem. Soc.* **1988**, *110*, 8385.
(4) Straatsma, T. P.; McCammon, J. A. *J. Chem. Phys.* **1989**, *91*, 3631.
(5) Dale, J.; Kristiansen, P. O. *J. Chem. Soc., Chem. Commun.* **1971**, 670.
(6) Buchanan, G. W.; Morat, C.; Ratcliffe, C. I.; Ripmeester, J. A. *J. Chem. Soc., Chem. Commun.* **1989**, 1306.
(7) Buchanan, G. W.; Kirby, R. A.; Ripmeester, J. A.; Ratcliffe, C. I. *Tetrahedron Lett.* **1987**, *28*, 4783.
(8) Watson, K. A.; Fortier, S.; Murchie, M. P.; Bovenkamp, J. W.; Rodrigue, A.; Buchanan, G. W.; Ratcliffe, C. I. *Can. J. Chem.* **1990**, *68*, 1201.
(9) Rothwell, W. P.; Waugh, J. S. *J. Chem. Phys.* **1981**, *74*, 2721.

0002-7863/92/1514-3294$03.00/0 Published 1992 by the American Chemical Society